Ultrasonics Sonochemistry 90 (2022) 106179

Contents lists available at ScienceDirect

Ultrasonics Sonochemistry

journal homepage: www.elsevier.com/locate/ultson

Facile preparation of graphene nitride by irradiating MHz ultrasound

Susumu Nii [a,*], Hiroki Ueda [a], Masami Aono [b], Kei Mizuta [a], Takashi Goshima [a]

[a] Dept. Chemical Engineering, Graduate School of Science and Engineering, Kagoshima University, 1-21-40 Korimoto, Kagoshima 890-0065, Japan
[b] Dept. Electrical and Electronics Engineering, Graduate School of Science and Engineering, Kagoshima University, 1-21-40 Korimoto, Kagoshima 890-0065, Japan

ARTICLE INFO

Keywords:
Ultrasonic
Graphene
Graphene nitride
High frequency

ABSTRACT

The present study aimed at developing a simple sonochemical method to prepare graphene nitride from the mixture of graphite and aqueous ammonia solution. Ultrasound of 1.6 MHz was irradiated to the sample in a fabricated sonoreactor at predetermined ultrasonic power and duration. The one-pot method succeeded in the preparation of graphene nitride. The generation was proven by XPS analysis in finding N1S peak in the spectrum. Detail analysis of N1s peak suggested that the major nitrogen species was pyrrolic type. Furthermore, the presence of CO bond proved the oxidation by OH radical. The reaction product had the value of N/C as high as 0.08, which is comparable to reported values for ultrasonic preparation of graphene nitride. The fact indicates that the significance of chemical effects of MHz range ultrasound, and the finding of the simple preparation method will accelerate practical application of graphene nitride.

1. Introduction

Graphene nitride attracts keen attention because of the potential applicability for catalysts [1–5] and semiconductors. Introducing nitrogen to graphite structure enables to control the bandgap [6] and also to change the electrical properties for semiconductors [7,8]. The two-dimensional structure is useful in the preparation of supercapacitors and also for photocatalyst in replacing TiO_2 [9,10]. Both increasing nitrogen content and controlling the composition of the type of nitride species alter the level of catalysis and capacitance. There are three types in graphene nitride, pyridinic, pyrrolic and graphitic. Guo [1] reported that graphitic nitrogen enhances electron transfer due to the neighbor carbon with Lewis base. The property improved the catalytic activity of electrode. A high content of pyrrolic nitrogen brought about a high capacitance for the efficient production of supercapacitors [11,12].

Because of the advantage, introduction of nitrogen to graphite structure, creation of the bond between C and N was extensively carried out both physically and chemically. The use of laser beam helps to introduce nitrogen at targeted position such as on the edges or in the specific part of the plane [13]. Plasma [11,14,15] or CVD [16] in nitrogen atmosphere was also applied to prepare graphene nitride. Most chemical methods use precursor of graphene oxide, GO. The preparation of GO requires a lot of operation steps and harsh chemicals. Further treatment of ultrasonication, hydrothermal treatment or heat annealing was carried out for nitridation [17]. Because of the simplicity in handling the feedstock and the product, chemical methods are potentially suitable for scaling-up of the production. Therefore, it is worth to explore an innovative chemical method for producing graphene nitride.

In a recent paper, Ida [17] reported that ultrasonication to GO in aqueous ammonia solution succeeded in the preparation of graphene nitride. The ultrasonic condition was 40 kHz, indirect irradiation, 200 W and 2 h. They proposed a mechanism for the nitridation of both OH radicals and ammonia radicals are playing their roles simultaneously. Their report stimulated us to explore the one-pot preparation method for graphene nitride with irradiating ultrasound. Instead of using GO, graphite is applied as a starting material. Ultrasound potentially enhances both oxidation and nitridation simultaneously.

In most of past works on ultrasonic application to prepare carbon materials, low frequency ultrasound such as 20 to 40 kHz was employed [17–20]. This is probably because of the expectation of exfoliation of graphite to prepare graphene and also the availability of the irradiation apparatus. Recently physical effects of MHz ultrasound were reported in the preparation of nanoemulsions [21,22] as well as the destructing microcapsules [23]. These physical effects come from both cavitation and high shear rate. The authors have a special interest on the application of MHz ultrasound to fields of chemical engineering such as ultrasonic atomization [24–34], emulsion splitting [35] and sonocrystallization [36]. Although there has been a recognition of less significant chemical effect for MHz-range ultrasound, generation of OH radicals are now frequently reported under irradiation of MHz

* Corresponding author.
E-mail address: niisus@cen.kagoshima-u.ac.jp (S. Nii).

https://doi.org/10.1016/j.ultsonch.2022.106179
Received 13 August 2022; Received in revised form 21 September 2022; Accepted 24 September 2022
Available online 26 September 2022

ultrasound [37–39]. Therefore, we expected the oxidation as well as the nitridation of graphite in the irradiation of MHz ultrasound. Furthermore, size of cavitation bubbles is much smaller than those under the irradiation of kHz ultrasound. Brotchie [40] reported that the resonance bubble diameter is approximately-one micrometer at 1 MHz. Those small bubbles are easy to access to finer spacings of solid materials to give physical and chemical effects of cavitation.

The objective of the present study is to develop the simple preparation method of graphene nitride by irradiating 1.6 MHz ultrasound. To pursue one-pot preparation, we choose the mixture of graphite and aqueous ammonia solution as the starting material. In a batch-type sonochemical reactor developed for the present study, the samples were treated with various irradiation time and ultrasonic power. The reaction product was analyzed with XPS for characterization.

2. Experimental

Reagent grade of graphite, potassium iodide, luminol, sodium carbonate and 10 % aqueous ammonia solution (FUJIFILM Wako Pure Chemical Co.) were used. Deionized waster was used to prepare KI and luminol solution. The batch-type sonochemical reactor was designed and fabricated for the present study. The main body of the reactor was a tube of stainless steel of I.D. 19 mm, which was equipped with two narrow branch tubes for setting liquid temperature sensor. On the bottom of the reactor, ultrasonic transducer of 1.64 MHz (HM-1630, Honda Electrics Co.) whose diameter was 18 mm was set on a thin stainless steel plate. The transducer was driven with the predetermined amplitude of voltage peak to peak from 0.1 to 0.5. K-type thermocouple was set inside each narrow tube to monitor the temperature of the liquid in the reactor. Prior to the ultrasonication to the samples, calorimetry was carried out using water to determine the ultrasonic power at the setting irradiation condition. A different glass reactor was used to observe sonochemical luminescence with using aqueous luminol solution of 5 % and Na_2CO_3. Pictures were taken to evaluate qualitatively for the generation of OH radicals. To quantify OH radical generation, KI oxidation was conducted with using 0.1 M aqueous KI solution. For safety reason, the highest working temperature in the sonochemical reactor was set at 343 K. Thus, all the experiment was conducted in the temperature range from 293 to 343 K. Twenty-five mL aqueous ammonia solution was poured into the reactor and 0.03 g of graphite was put into the solution. Ultrasound of 1.64 MHz was irradiated to the mixture at predetermined duration and ultrasonic power. The reaction product was transferred to a glass vial for observation and storage. Since ultrasonication helps to break down or to exfoliate graphite into fine particles, samples show different turbidity depending on the condition. Thus, sedimentation test was conducted to compare the physical effect of ultrasound on graphite.

For characterization, X-ray photo electron spectroscopy (XPS; Shimadzu AXIS-ULTRA DLD). The sample was prepared by dropping the samples on the glass substrate. Samples were analyzed after drying the substrates with samples at ambient atmosphere. The atomic concentration was determined from the area ratio of N1s spectra to C1s spectra and O1s spectra.

3. Results and discussion

3.1. OH radical generation in the sonoreactor

Fig. 1 shows the sonochemicl luminescence observed under the irradiation of 1.6 MHz and 15 W of ultrasonic power. Appeared was an inclined column of bright blue to white colored. The inclination was due to the angled setting of the transducer. In the right end side, white part shows the reflection at the sound on the top liquid surface. The luminescence clearly shows the occurrence of OH radicals in the sonoreactor. At a similar frequency of 1.1 MHz, Kauer et al., also reported SCL near a solid wall[41]. Our finding of the presence of bright-column zone is an important fact to stress because the generation of OH radical assures the validity of our attempt of applying 1.6 MHz ultrasound for the development of a sonoreactor.

Fig. 1. Sonochemiluminescence under 1.6 MHz and 15 W in reactor.

Result of calorimetry was shown in Fig. 2. The working amplitude of the electric signal, voltage peak to peak was varied from 0.1 to 0.5. Calorimetry was conducted using deionized water. The ultrasonic power was calculated on the basis of the slope of temperature change with time, and the values were plotted in Fig. 2 against volt peak to peak. The plot gives us the energy input to the sample mixture.

Fig. 3 shows the generation rate of triiodide ion from aqueous KI solution. Since the amount of triiodide ion corresponded to the amount of OH radical, the generation rate is regarded to as that of OH radical. It linearly increased with increasing ultrasonic power. Therefore, it was proven that the developed reactor produces considerable amount of OH radicals at the present irradiation condition. The result provides a solid base for our extraordinary idea of a sonoreactor working under MHz ultrasound.

3.2. Sedimentation test

Fig. 4 represents the result of sedimentation test of samples applied at three different irradiation conditions. Details of the conditions are given in the figure caption. Before taking pictures, samples in vials were

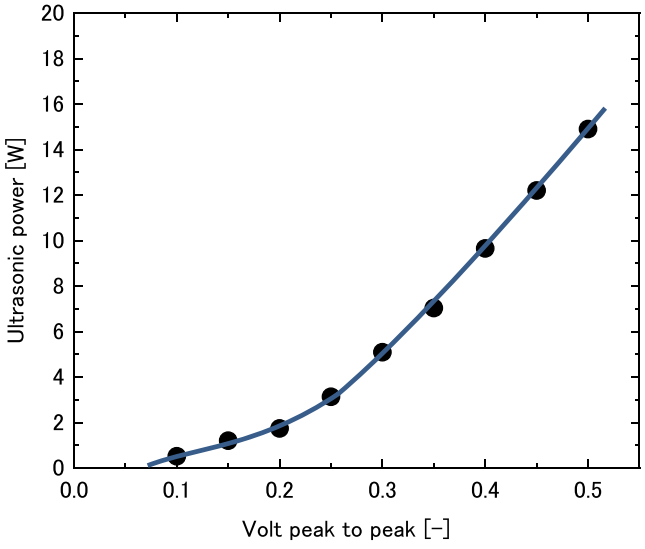

Fig. 2. Ultrasonic power against voltage amplitude (voltage peak to peak).

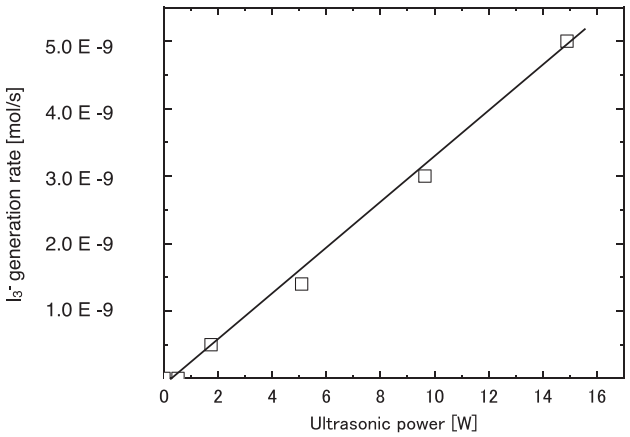

Fig. 3. I_3^- generation rate against ultrasonic power.

shaken vigorously by hand for a minute and stood still. To ensure the reproducibility of the test, the sedimentation experiment was repeated more than three times. Little difference in the change of turbidity with time was observed with naked eye. Pictures were taken at 0 and 150 min to observe the dispersion state of fine particles in liquid. The lowest ultrasonic power of 7.7 W and 30 min irradiation resulted in quick sedimentation of particles. Number 2, ultrasonic power of 14 W and 30 min irradiation yielded the darkest dispersion among the three samples. The result suggests the physical effect of MHz frequency is effectively working and it enhances breaking down of graphite particles. Interestingly, the color in the liquid for the sample No. 3 was clearer than that of No. 2. The fact suggested that the higher ultrasonic power works more effective in breaking down of graphite particles than longer time irradiation. It should be noted that the trend is limited to the observable size of particle with naked eye. For smaller scale particles unobservable with naked eye, further characterization is required.

3.3. XPS analysis

Fig. 5 shows XPS spectra of the sample obtained on the condition of ultrasonic power of 10 W and irradiation time for 15 min. Significantly, N1s peak, which is the evidence of carbon nitride, appeared in the range of 397 to 401 eV. Significantly, the fact proved irradiation of 1.6 MHz ultrasound works effectively to nitridation of graphite with the simple preparation condition of mixing graphite and ammonia solution. It is worth to describe our preliminary experimental result of irradiating 40 kHz ultrasound to the mixture of graphite and 10 wt% ammonia solution in a vial. Indirect ultrasonic irradiation was conducted with a bath-type sonicator at input power of 70 W for different irradiation time ranging from 30 to 120 min. XPS analysis of the samples showed negligibly small peaks in the range of 397 to 401 eV. Therefore, the appearance of N1s peak is specifically due to the irradiation of 1.6 MHz ultrasound. Expanded spectrum of N1 peak was shown in Fig. 6. Since the main peak is close to pyrrolic N which was assigned to 399.7 eV, the major nitrogen species is pyrrolic type. Interestingly, the result accorded to the report by Ida et al., where they used GO as a starting material and 40 kHz

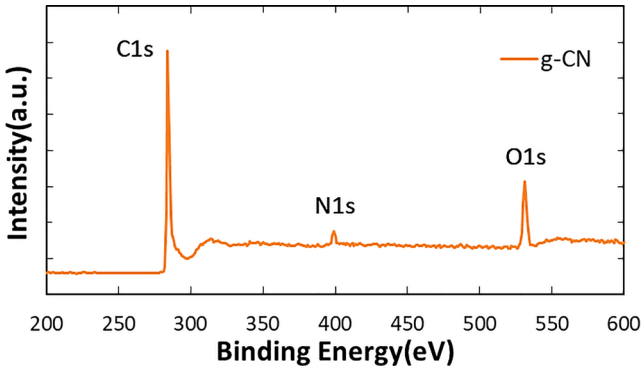

Fig. 5. XPS spectra of graphene nitride.

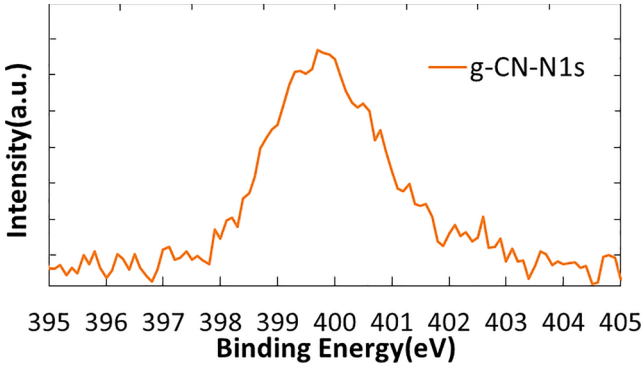

Fig. 6. Expanded spectrum of N1s peak.

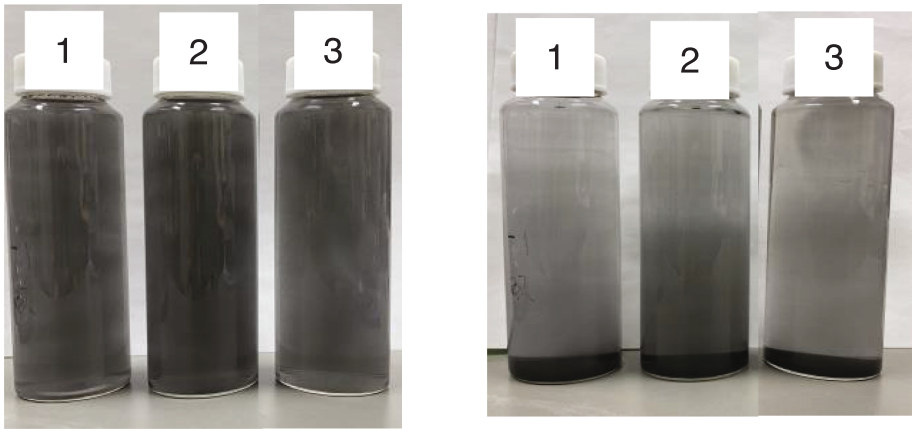

Fig. 4. Progress of sedimentation with time from (a) to (b) for samples prepared at different ultrasonic conditions, No.1: 7.7 W, 30 min., No.2: 14 W, 30 min, No.3: 7.7 W, 120 min.

ultrasound. There can be a similar working mechanism for MHz ultrasound in fabricating graphene nitride.

Fig. 7 shows convolution results of C1s peak. For nitrogen peaks, sp2C-N and sp3C-N were observed, which are fingerprints of *N*-doping. Also, the presence of C═O peak suggests that the oxidation with OH radical.

A special care should be taken in the interpretation of O1s peak as a result of oxidation. The use of glass substrate for XPS analysis resulted in the inclusion of the effect of SiO_2 to the observed O1s peak signal. Therefore, it should be removed to evaluate the progress of oxidation. As was presented in Fig. 8, effect of CO bond was obtained from the peak convolution. The quantitative evaluation of oxygen introduction resulted in the elemental percent of 6. 46.

According to the peak analysis of XPS spectrum, elemental ratio was calculated and tabulated in Table 1. Significantly, the percentage of nitrogen reached 3.69 which is higher than 3.46, the reported values of Tao et al. for the irradiation of 40 kHz to the mixture of GO and aqueous ammonia solution at 5 degree C [5].

3.4. Comparison of N/C values at different irradiation conditions

Experiments of graphite nitridation were performed on the conditions of various ultrasonic power and duration to explore a better condition for higher N/C values. Ultrasonic power was changed from 2.2 to 16 W and irradiation time was set at 15, 30, 60 and 90 min. Several combinations of ultrasonic power and duration of the irradiation were examined and results of N/C values were plotted in Fig. 9. On the horizontal axis, taken was the calculated amount of I_3^- to be generated at the setting condition. The amount was given by multiplying I_3^- generation rate presented in Fig. 3 at applied ultrasonic power and duration of irradiation. It corresponds to the amount of OH radical generated. N/C values increased with increasing the amount of I3-. The highest value of N/C was 0.080 at 16 W, which is the highest ultrasonic power in a relatively short period of time of 30 min. At slightly lower ultrasonic power of 8.9 W, a similar N/C value was obtained in a longer irradiation time of 60 min. Extension of irradiation time to 90 min at 9.0 W of ultrasonic power resulted in a lower N/C value than the highest one. This result suggested that too long ultrasound irradiation was less effective to increase N/C value, which might be caused by partial degradation of carbon nitride. Due to the influence of irradiation time on nitridation, N/C values are obviously affected by multiple parameters of ultrasonic power and irradiation time. Therefore, horizontal axis of Fig. 9 was taken with values corresponding to the multiplication of ultrasonic power and time.

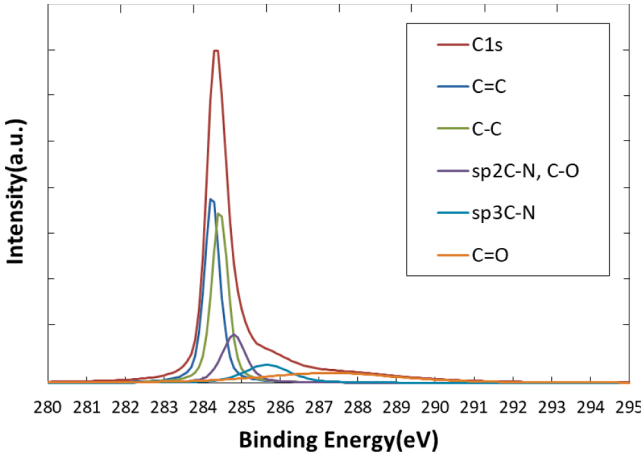

Fig. 7. Peak convolution of C1s spectrum.

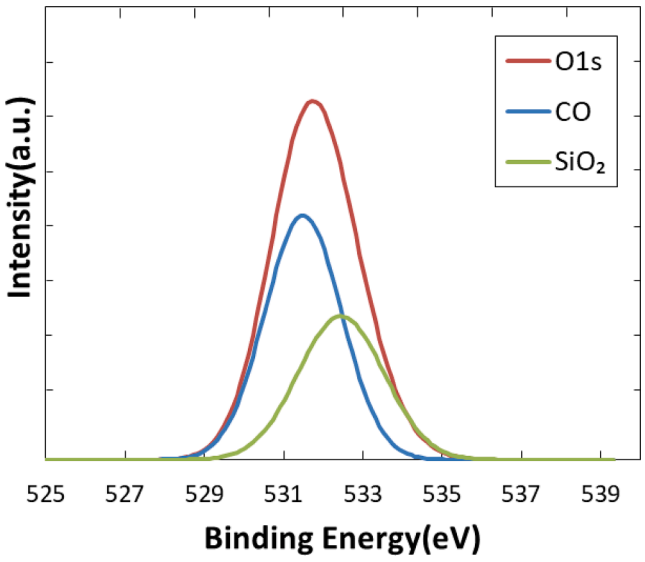

Fig. 8. Peak convolution of O1s spectrum.

Table 1
Percentage of element and elemental ratio.

C [atomic %]	N [atomic %]	O [atomic %]	N/C [-]
89.85	3.69	6.46	0.0411

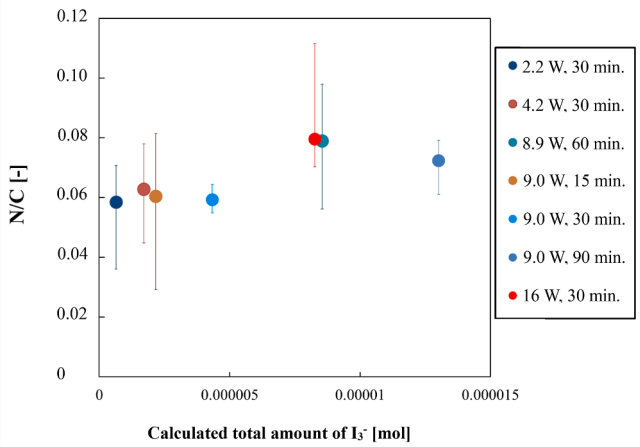

Fig. 9. Change of N/C values against calculated amount of total OH radical.

4. Conclusion

The present study proved that application of MHz ultrasound successfully works to prepare graphene nitride by irradiating the ultrasound to the mixture of graphite and 10 % ammonia solution. The XPS analysis reveals N1s peak which is evidence for the substitution of carbon atom with nitrogen atom in graphite plane. Detail analysis of N1s peak suggests that pyrrolic-N was the dominant nitrogen species. Significance of the present study is twofold. One is a development of a sonoreactor driven with MHz ultrasound. It produced enough amount of OH radical for the preparation of graphene nitride. The amount of OH radical was quantified with KI oxidation. The other is to find a simple route in the preparation of graphene nitride without using graphene oxide as a precursor. The reaction product had the value of N/C as high as 0.08, which is comparable to reported values obtained with ultrasonic irradiation to the mixture containing GO at 40 kHz. Effect of irradiation

conditions on nitridation was examined under various irradiation conditions. The value of N/C increased with increasing ultrasonic power as well as irradiation time. However, the longer irradiation resulted in a slight decrease of N/C value.

CRediT authorship contribution statement

Susumu Nii: Conceptualization, Writing – review & editing, Supervision. **Hiroki Ueda:** Investigation, Methodology. **Masami Aono:** Investigation, Methodology. **Kei Mizuta:** Visualization, Writing – review & editing. **Takashi Goshima:** Writing – review & editing.

Declaration of Competing Interest

The authors declare that they have no known competing financial interests or personal relationships that could have appeared to influence the work reported in this paper.

Data availability

Data will be made available on request.

Acknowledgement

We thank to Mr. Yuto Kubo for his effort in carrying out the XPS analysis.

References

[1] D. Guo, R. Shibuya, C. Akiba, S. Saji, T. Kondo, J. Nakamura, Active sites of nitrogen-doped carbon materials for oxygen reduction reaction clarified using model catalysts, Science 351 (6271) (2016) 361–365.
[2] H. Miao, S. Li, Z. Wang, S. Sun, M. Kuang, Z. Liu, J. Yuan, Enhancing the pyridinic N content of Nitrogen-doped graphene and improving its catalytic activity for oxygen reduction reaction, Int. J. Hydrogen Energy 42 (47) (2017) 28298–28308.
[3] N. Candu, I. Man, A. Simion, B. Cojocaru, S.M. Coman, C. Bucur, A. Primo, H. Garcia, V.I. Parvulescu, Nitrogen-doped graphene as metal free basic catalyst for coupling reactions, J. Catal. 376 (2019) 238–247.
[4] Y. Bian, H. Wang, J. Hu, B. Liu, D. Liu, L. Dai, Nitrogen-rich holey graphene for efficient oxygen reduction reaction, Carbon 162 (2020) 66–73.
[5] H. Tao, C. Yan, A.W. Robertson, Y. Gao, J. Ding, Y. Zhang, T. Ma, Z. Sun, N-doping of graphene oxide at low temperature for the oxygen reduction reaction, Chem. Comm. 53 (2017) 873.
[6] P. Rani, V.K. Jindal, Designing band gap of graphene by B and N dopant atoms, RSC Adv. 3 (2013) 802–812.
[7] J. Yang, W. He, Q. Jiang, Z. Chen, H. Ju, X. Xue, Z. Xu, P. Hu, G. Yu, Hydrogen-dominated metal-free growth of graphitic-nitrogen doped graphene with *n*-type transport behaviors, Carbon 161 (2020) 123–131.
[8] M. Wimalanandaa, J.K. Kim, S.W. Cho, J.M. Lee, Highly efficient two-step nitrogen doping of graphene oxide-based materials in oxygen presence atmosphere for high-performance transistors and electrochemical applications, J. Sci.: Adv. Mater. Devices 7 (2022), 100481.
[9] Y. Huo, J. Zhang, K. Dai, Q. Li, J. Lv, G. Zhu, C. Liag, All-solid-state artificial Z-scheme porous g-C_3N_4/Sn_2S_3-DETA heterostructure photocatalyst with enhanced performance in photocatalytic CO_2 reduction, Appl. Chatl. B: Environ. 241 (2019) 528–538.
[10] X. Li, J. Zhang, Y. Huo, K. Dai, S. Li, S. Chen, Two-dimensional sulfur- and chlorine-codoped g-C_3N_4/CdSe-amine T heterostructures nanocomposite with effective interfacial charge transfer and mechanism insight, Appl. Catal. B: Environ. 280 (2021), 119452.
[11] H. Sun, Q. Wang, T. Wu, Y. Miao, Y. Fang, Plasma-assisted synthesis of pyrrolic-nitrogen doped reduced graphene oxide to enhance supercapacitor performance, Appl. Surf. Sci. 527 (2020), 146574.
[12] H.M. Jeong, J.W. Lee, W.H. Shin, Y.J. Choi, H.J. Shin, J.K. Kang, J.W. Choi, Nitrogen-doped graphene for high-performance ultracapacitors and the importance of nitrogen-doped sites at basal planes, Nano Letters 11 (6) (2011) 2472–2477.
[13] W. Zheng, Y. Zhang, K. Niu, T. Liu, K. Bustillo, P. Ercius, D. Nordlund, J. Wu, H. Zheng, X. Du, Selective nitrogen doping of graphene oxide by laser irradiation for enhanced hydrogen evolution activity, Chem. Commun. 97 (2018).
[14] M. Rybin, A. Pereyaslavtsev, T. Vasilieva, V. Myasnikow, I. Sokolv, A. Pavlova, E. Obraztsova, A. Khomich, V. Ralchenko, E. Obraztsova, Efficient nitrogen doping of graphene by plasma treatment, Carbon 96 (2016) 196–202.
[15] G.R. Bigras, X. Glad, L. Vandsburger, C. Charpin, P. Levesque, R. Martel, L. Stafford, Low-damage nitrogen incorporation in graphene films by nitrogen plasma treatment: Effect of airborne contaminants, Carbon 144 (2019) 532–539.
[16] G. Imamura, K. Saiki, Synthesis of nitrogen-doped graphene on Pt(111) by chemical vapor deposition, J. Phys. Chem. C 115 (2011) 10000–10005.
[17] S. Ida, P. Wilson, B. Neppolian, M. Sathish, P. Karthik, P. Ravi, Ultrasonically aided selective stabilization of pyrrolic type nitrogen by one pot nitrogen doped and hydrothermally reduced Graphene oxide/Titania nanocomposite (N-TiO_2/N-RGO) for H_2 production, Ultrason. Sonochem. 57 (2019) 62–72.
[18] D. Wang, W. Hu, Q. Ma, X. Zhang, X. Xia, H. Chen, H. Liu, Nitrogen-containing graphene networks with high volumetric capacitance and exceptional rate capability, Carbon 154 (2019) 13–23.
[19] G. Lemes, D. Sebastián, E. Pastor, M.J. Lázaro, N-doped graphene catalysts with high nitrogen concentration for the oxygen reduction reaction, J. Power Sources 438 (2019), 227036.
[20] I.L. Alonso-Lemus, M.Z. Figueroa-Torres, A.B. García-Hernández, B. Escobar-Morales, F.J. Rodríguez-Varela, A.F. Fuentes, D. Lardizabal-Gutierrez, P. Quintana-Owen, Low-cost sonochemical synthesis of nitrogen-doped graphene metal-free electrocatalyst for the oxygen reduction reaction in alkaline media, Inter. J. Hydro Energy 42 (2017) 30330–30338.
[21] K. Nakabayashi, F. Amemiya, T. Fuchigami, K. Machida, S. Takeda, K. Tamamitsu, M. Atobe, Highly clear and transparent nanoemulsion preparation under surfactant-free conditions using tandem acoustic emulsification, Chem. Commun. 20 (2011) 5765–5767.
[22] T. Nemoto, T. Sakai, T. Okada, Unimodal sized silica nanocapsules produced through water-in-oil emulsions prepared by sequential irradiation of kilo- and submega-hertz ultrasounds, RSC Adv. 11 (2021) 22921–22928.
[23] A. Inui, A. Honda, S. Yamanaka, T. Ikeno, K. Yamamoto, Effect of ultrasonic frequency and surfactant addition on microcapsule destruction, Ultrason. Sonochem. 70 (2021), 105308.
[24] Y. Ono, K. Sekiguchi, K. Sankoda, S. Nii, N. Namiki, Improved ultrasonic degradation of hydrophilic and hydrophobic aldehydes in water by combined use of atomization and UV irradiation onto the mist surface, Ultrason. Sonochem. 60 (2020), 104766.
[25] T. Kudo, K. Sekiguchi, K. Sankoda, N. Namiki, S. Nii, Effect of ultrasonic frequency on size distributions of nanosized mist generated by ultrasonic atomization, Ultrason. Sonochem. 37 (2017) 16–22.
[26] S. Nii, N. Oka, Size-selective Separation of Submicron Particles in Suspensions with Ultrasonic Atomization, Ultrason. Sonochem. 21 (2014) 2032–2036.
[27] K. Suzuki, J. Hisaeda, S. Nii, Application of ultrasonic atomization for fractionating particles from suspensions, J. Chem. Eng. Jpn. 45 (2) (2012) 114–118.
[28] K. Suzuki, D.M. Kirpalani, S. Nii, Influence of cavitation on ethanol enrichment in an ultrasonic atomization system, J. Chem. Eng. Jpn. 44 (9) (2011) 616–622.
[29] S. Nii, M. Toki, S. Watanabe, K. Suzuki, K. Matsuura, T. Fukazu, Ethanol separation through ultrasonic atomization under controlled pressure, J. Chem. Eng. Jpn. 43 (1) (2010) 99–103.
[30] K. Matsuura, S. Nii, T. Fukazu, K. Tsuchiya, Efficient reduction of gasoline volatility through ultrasonic atomization, Ind. Eng. Chem. Res. 46 (2007) 2231–2234.
[31] S. Nii, K. Matsuura, T. Fukazu, M. Toki, F. Kawaizumi, A novel method to separate organic compounds through ultrasonic atomization, Chem. Eng. Res. Des. 84, A5 (2006) 412-415.
[32] K. Suzuki, K. Arashi, S. Nii, Determination of droplet and vapor ratio of ultrasonically-atomized aqueous ethanol solution, J. Chem. Eng. Jpn. 45 (5) (2012) 337–342.
[33] H. Takaya, S. Nii, F. Kawaizumi, K. Takahashi, Enrichment of surfactant from its aqueous solution using ultrasonic atomization, Ultrason. Sonochem. 12 (2005) 483–487.
[34] S. Nii, S. Kikumoto, H. Tokuyama, Quantitative approach to ultrasonic emulsion separation, Ultrason. Sonochem. 16 (1) (2009) 145–149.
[35] S. Nii, S. Takayanagi, Growth and size control in anti-solvent crystallization of glycine with high frequency ultrasound, Ultrason. Sonochem. 21 (2014) 1182–1186.
[36] H. Harada, N. Iwata, K. Shiratori, Observation of multibubble sonoluminescence from water saturated with various gases during ultrasonic atomization, Jpn. J. Appl. Phys. 48 (2009) 07GH01-1–07GH01-4.
[37] J. Frohly, S. Labouret, C. Bruneel, I. Looten-Baquet, R. Torguet, Ultrasonic cavitation monitoring by acoustic noise power measurement, J. Acoust. Soc. Am. 108 (2000) 2012–2020.
[38] N. Segebarth, O. Eulaerts, J. Reisse, L.A. Crum, T.J. Matula, Correlation between acoustic cavitation noise, bubble population and sonochemistry, J. Phys. Chem. B 106 (2002) 9181–9190.
[39] A. Brotchie, F. Grieser, M. Ashokkumar, Effect of power and frequency on bubble-size distributions in acoustic cavitation, Physical Review Letters, PRL 102 (2009), 084302.
[40] M. Kauer, V. Belova-Magri, C. Cairos, H. Schreier, R. Mettin, Visualization and optimization of cavitation activity at a solid surface in high frequency ultrasound fields, Sonochem, Ultrason., 2017, pp. 474–483.